Available online at www.sciencedirect.com

ScienceDirect

Procedia Engineering 213 (2018) 691–698

Procedia Engineering

www.elsevier.com/locate/procedia

7th International Conference on Fatigue Design, Fatigue Design 2017, 29-30 November 2017, Senlis, France

High cycle fatigue strength assessment methodology considering punching effects

Helmi Dehmani[a]*,Charles Brugger[b], Thierry Palin-Luc[b], Charles Mareau[c], Samuel Koechlin[a]

[a] *Nidec-Leroy Somer, Boulevard Marcellin Leroy, Angoulême, France*
[b] *Arts et Métiers ParisTech, I2M, CNRS, Esplanade des Arts et Métiers, Talence, France*
[c] *Arts et Métiers ParisTech, LAMPA, Boulevard du Ronceray, Angers, France*

Abstract

Since a decrease of the fatigue strength may result from punching operations, this study proposes a methodology for designing punched parts against high cycle fatigue crack initiation. To reach this goal, high cycle fatigue tests are performed on different specimens configurations with either punched or polished edges. Due to punching effects, the fatigue strength of punched specimens is significantly decreased. Fracture surfaces observations reveal that crack initiation occurs always on a punch defect. Additional investigations are combined to characterize how the edges are altered by the punching operations. High tensile residual stress levels along the loading direction are quantified using X-Ray diffraction techniques. Furthermore, micro-hardness measurements and X-Ray diffraction results reveals a strong hardness gradient due to punching operation. For a better understanding of crack initiation mechanisms, the edge geometries have been scanned with 3D optical microscopy, allowing us to identify the most critical defect (and its real geometry) by comparing the edges before and after fatigue failure. Finally, FEA are performed on identified defects. A non-local high cycle multiaxial fatigue strength criterion has been used as post-processing of FEA to take into account the effect on the HCF strength of defects and the strong stress-strain gradients around them.

Peer-review under responsibility of the scientific committee of the 7th International Conference on Fatigue Design.

Keywords: Fe-Si, high cycle fatigue, punching effect, defect, residual stress, gradient effect

* Corresponding author. Tel.: +33 5 45 64 54 62.
E-mail address: helmi.dehmani@mail.nidec.com

1877-7058
Peer-review under responsibility of the scientific committee of the 7th International Conference on Fatigue Design.
10.1016/j.proeng.2018.02.065

1. Introduction

New electric motors generations require high-performance electrical steel sheets. These materials, which present better magnetic properties, are suitable for several applications especially high speed electric motors. The improved magnetic properties of Fe-Si alloys are provided by reducing thickness, adjusting silicon content and increasing the grain size. Electric motors are made from stacks of thin sheets. Punching process is usually used to produce these components because it offer a good production rate and low cost. However, this process generates different effects influencing the durability of components. Several studies have highlighted the influence of these effects which are hardening, tensile residual stresses and defects [1–4]. In order to study the effect of punching process on the high cycle fatigue strength of electric motor components and to take into account these effects when designing pieces, an experimental and numerical procedure are curried out. Fatigue tests have been performed on different specimen's configurations. Punched, polished and punched-annealed specimens are used to quantify the contribution of each effect induced by the process on the high cycle fatigue strength of the studied alloy. SEM observations reveal that fatigue crack initiation occurs on the specimen's edge. In order to study the fatigue crack initiation mechanisms, SEM observations and 3D surface topography of the specimens have been performed. Results show damaged edges with many types of defects. A specific procedure is used to identify the critical defects [5-6]. X-Ray diffraction techniques are used to analyze residual stresses distribution after punching. Moreover, micro-hardness measurements and X-Ray diffraction techniques are used to characterize the depth of the hardened zone due to punching process. These investigations show an important gradient of the mechanical properties a high residual stress level and geometrical defects generated by the punching operation. To have a reliable estimation of the fatigue resistance of these components, a finite element model has been developed to account for the influence of the punched edge and the defects on the HCF strength of punched components. A non-local high cycle multiaxial fatigue strength criterion has been used as post-processing of FEA to consider the effect of defects and the strong stress-strain gradients around them.

Consequently this paper is to propose a fatigue design strategy for electric motor components taking into account the effects of geometrical defects.

2. Experimental procedure

The studied material is M330-35A electrical steel delivered in the form of rolled sheets with a nominal thickness of 350 μm. Metallographic observations reveal an equiaxed microstructure with a mean grain size of 100 μm. Chemical composition is given in Table 1. Monotonic tensile tests have been performed on specimens obtained from three different directions in the sheet plane. Results show that the maximal difference for the yield stress is about 7%. As a consequence, in the following, mechanical properties are considered to be isotropic.

Table 1. Chemical composition of the studied alloy

Element	Si	Mn	Al	Fe
%	2-3.5	0.5-0.6	0.4-1.2	95-98

High cycle fatigue tests have been performed in air under uniaxial tension loading along the rolling direction, using a resonant fatigue testing machine (Vibrophore type) at a frequency of about 65 Hz. Tests were carried out under load control on smooth specimens at room temperature (≈20°C) using R=0.1 loading ratio. A parallel edge geometry with a calibrated zone was used for fatigue tests. It allows cut edge defects to be critical whatever their position along the 20 mm gauge length. The stop criterion was a frequency drop of 1 Hz, which corresponds to the total specimen's failure, or when the maximum number of cycles (5×10^6 cycles) was reached. In order to quantify the contribution of each effect induced by the punching process on the fatigue resistance of this Fe−Si alloy, different specimen configurations were tested:

- (C1) Punched specimens
- (C2) Punched then polished specimens

- (C3) Punched then annealed specimens
- (C4) Punched then polished then annealed specimens

To obtain polished specimens, a mechanical polishing was done using silicon carbide papers from P1200 to P4000 grades until all the visible defects were removed. Polishing operations are expected to modify the hardening and the residual stress distribution initially induced by punching. Moreover, in order to relieve residual stresses and to eliminate hardening induced by punching, an annealing treatment was applied to some specimens in a controlled environment. As a consequence of this treatment, a local recrystallized region, which is about 50 µm deep, is observed for punched and annealed specimens. In this region, the initial large grains are thus transformed into small grains with no hardening.

3. Fatigue tests results

3.1. S-N curves

The S–N curves corresponding to the different specimen configurations are presented in Fig. 1. The punched−polished−annealed configuration (C4) is taken as reference to quantify the contribution of the different effects induced by the punching process.

All the effects of the punching process are related to C1 specimens. Results show a drop of 20% on the median fatigue strength at 5×10^6 cycles. The effect of punching defects (geometric effect only) is then investigated. A drop of 8% is observed in the case of C3 specimens. But an increase of 11% of the fatigue resistance is observed for C2 specimens. This represents the positive effect of the mechanical polishing process (defects removes but residual stresses modified). However, for high stress levels, the difference between configurations is reduced since fatigue crack initiation is governed by the specimen macroscopic plasticity.

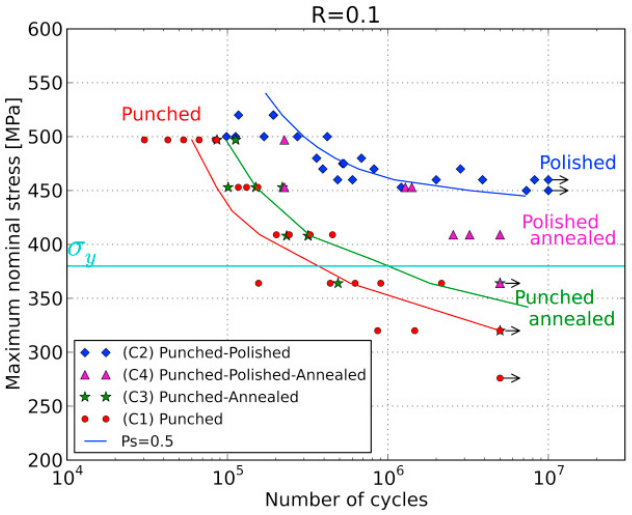

Fig. 1. S-N curves obtained for different specimen's configurations

3.2. Fracture surfaces observations

To identify the crack initiation mechanisms, SEM observations of the fracture surfaces have been performed for different specimen's configurations (Fig. 2). For punched (C1) and punched−annealed (C3) specimens, initiation occurs on edge on a punch defect. However, for punched−polished specimens (C2) initiation in most of the cases is

transgranular. Since crack initiation mechanism is strongly depending on the nature of the edge, additional investigations are carried out in order to study the effect of the process on fatigue crack initiation.

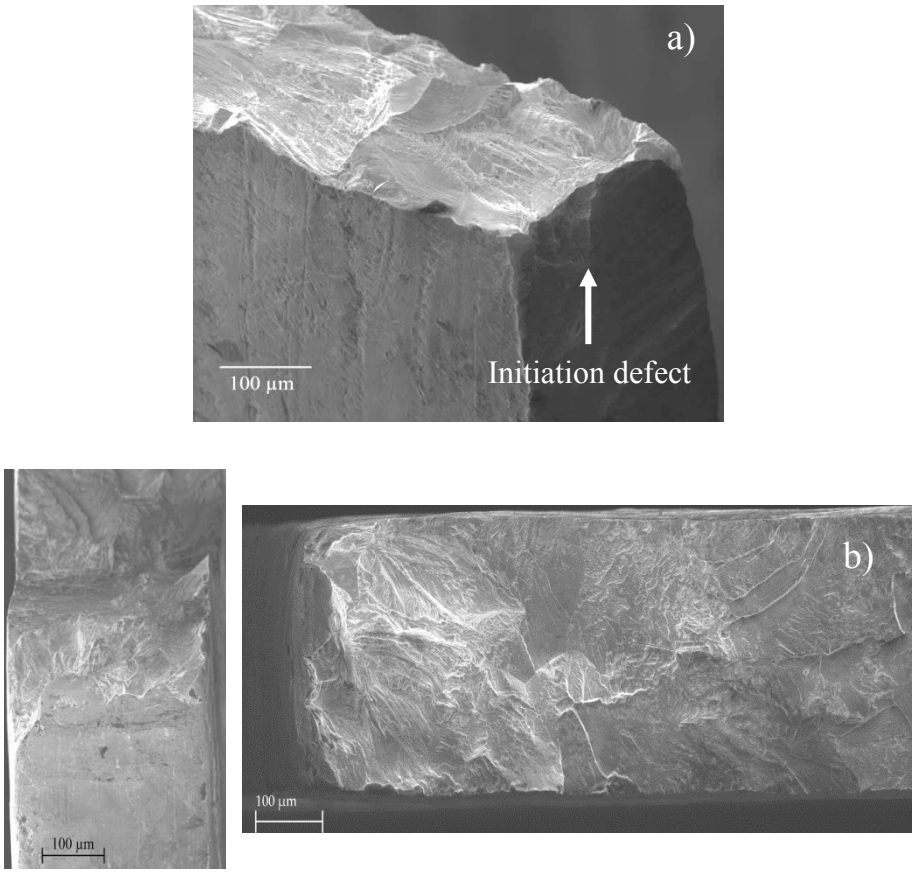

Fig. 2. SEM observations of fracture surfaces: initiation defect for (a) punched specimens (C1) (b) and (c) polished specimens (C2)

4. Discussion

4.1. Micro-hardness measurements

To determine the depth of the layer affected by the punching and polishing operations, micro-hardness measurements (HV 0.1) were performed on some specimens from the C1, C2 and C3 configurations. Measurements were performed starting from the specimen's edge. For punched specimens results show a gradient of the material properties gradient until a distance of 200 µm. The hardening layer depth is then about 200 µm. For punched−polished specimens, micro-hardness values are comparable to the value of the material without any process effect.

Measurements are performed on punched−annealed specimens. Results show that the hardening, layer initially introduced by punching, is removed after annealing treatment.

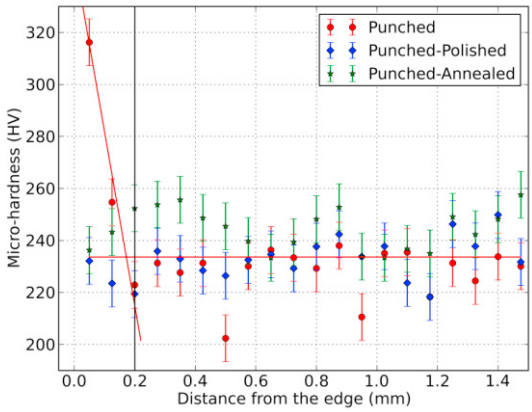

Fig. 3. Micro-hardness measurements for different specimen's configurations (vertical bars represent experimental uncertainty)

4.2. XRD analyses

X-ray diffraction techniques offer a better resolution for estimating the hardened depth. In the present work, because of the low sheet thickness, analyses were performed on a stack of 10 sheets. Each stress value was estimated on an irradiated zone which approximately corresponds to a 2 mm diameter disk. Residual stresses were determined first on punched edges, then on surfaces obtained after successive layer removal operations using electrochemical polishing techniques. Analyses were conducted for C1, C2 and C3 specimens. The results relative to the in-depth evolution of the longitudinal residual stresses σ_{yy} are shown in Fig. 4a. Punched specimens exhibit high tensile residual stresses. However, for punched−polished specimens (C2), important compression residual stresses exist on edges. For punched−annealed specimens (C3), residual stress analyses were performed only on edges (zero depth). Results show that the high tensile residual stresses initially induced by punching are fully relieved after the annealing treatment.

The Full Width at Half Maximum (FWHM) provides a qualitative evaluation of hardening. The evolution of the FWHM, associated with X-ray analyses, as a function of depth is plotted for C1, C2 and C3 specimens in Fig. 4b. The maximum value is obtained on the top surface of the edge then values decrease and stabilize with an increasing depth. For punched specimens, the results show that the depth affected by punching operations is about 200 µm, which is consistent with micro-hardness measurements.

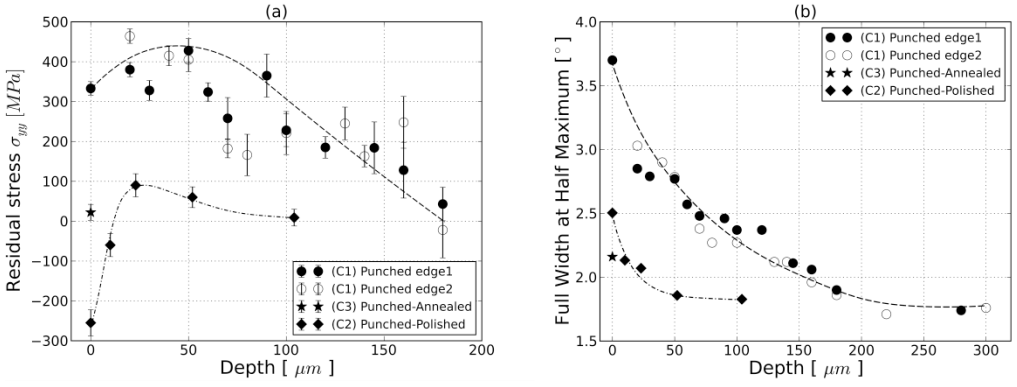

Fig. 4. (a) Longitudinal normal residual stress σ_{yy} profile for punched, punched-polished and punched-annealed specimens (b) Full Width at Half Maximum relative to X-ray analyses

4.3. SEM observations and 3D surface topography

Since fracture surface observations reveals that fatigue crack initiation occurs on a defect located in the specimen edge, SEM observations and 3D surface topography of punched specimens are performed. A damaged edge with 4 zones (typically found on the punched edges) is observed [3–5]. The largest defects are located in the fracture zone. The 3D geometry of the edge is obtained from the scan data. A specific procedure used to identify the critical defect is detailed in [5-6]. Some critical defect geometries used for FEA are presented in Fig.5. The objective is to obtain the stress and strain distribution around the defect.

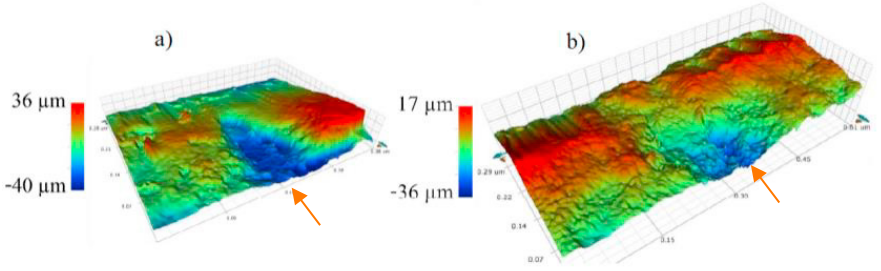

Fig. 5. Critical defect identified for (a) first specimen; (b) second specimen.

5. FEA considering the effect of defects

5.1. FE simulations

To consider the geometrical effect of punching defects, finite elements analyses are performed on real defect geometries. Six critical defect geometries are used. To ensure the mesh convergence and to optimize the simulation time, a mesh dimension sensitivity study is performed. An element size of 5 µm along the X and Y directions and 10 µm along the Z direction was finally chosen. Because fatigue tests were conducted in the high cycle regime, the applied stress levels (for R=0.1 loading ratio) are less than the material yield stress. However, an elastic-plastic constitutive model with linear isotropic hardening rule is used for simulations to take into account plasticity around defects [6-7]. The material model parameters were identified from the results of low cycle fatigue tests carried out on the studied alloy under load control [6-7]. Since stress-based fatigue criterions were used to assess the fatigue resistance of components. Simulations are performed until reaching a stabilized stress state.

5.2. Fatigue strength assessment using local and non-local HCF criterion

The post-processing of FEA was performed using Crossland local [8] and non-local [9-10] HCF criterion.

$$Local\ criterion \quad : \sigma_{éq}^{Cr} = \tau_{oct,a} + \alpha_{cr}\sigma_{H,max} \leq \beta_{cr} \tag{1}$$

$$Non-local\ criterion : \langle \sigma_{éq}^{Cr} \rangle = max_{P\in V}\left[< \tau_{oct,a} > + \alpha_{cr}\alpha < \sigma_{H,max} > \right] \leq \beta_{cr} \tag{2}$$

With:

$$< \tau_{oct,a} >= \frac{1}{V_a} \iiint_{Va} \tau_{oct,a}\, dV \tag{3}$$

$$< \sigma_{H,max} >= \frac{1}{V_a} \iiint_{Va} \sigma_{H,max}\, dV \tag{4}$$

The threshold relative to C4 specimens, which represents the material without any influence of the process, is used for evaluating the Crossland criterion. For the non-local approach, the critical distance *dc* was optimized on one critical defect geometry in order to have an averaged danger coefficient close to 1. The averaging distance was optimized at 45 µm which can be related to defect size. The points representing the shear stress amplitude versus the maximal hydrostatic stress calculated at the integration points of the FE model are plotted in the Crossland diagram (Fig. 6a) for a critical defect. Points are calculated using the local and the non-local Crossland approaches. Comparative study was performed on different critical defect geometries using the two approaches. Results are presented in the histogram (Fig. 6b). The same critical distance, identified on one defect geometry, was used for all the other defects.

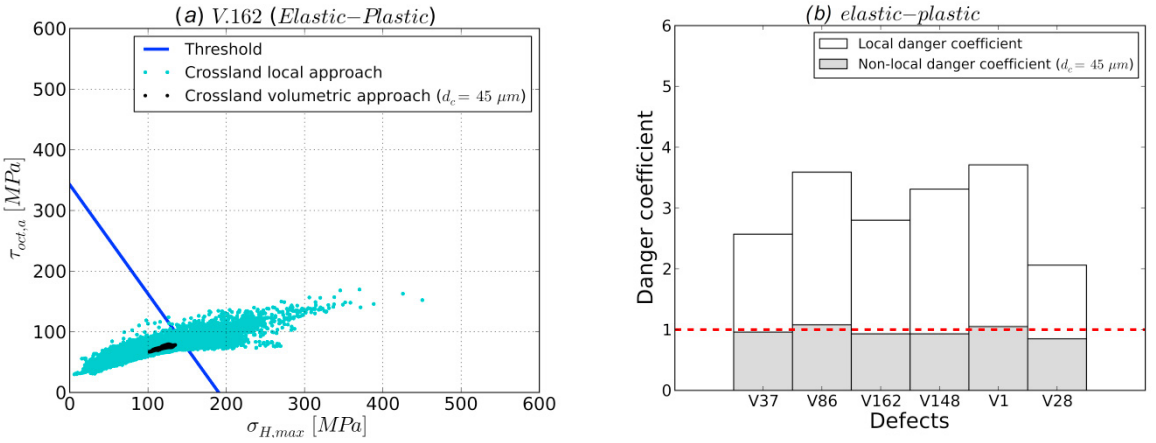

Fig. 6. (a) Comparison between local and non-local Crossland diagram formulations for an identified critical defect (b) Histogram of danger coefficients for different critical defect calculated using local and non-local Crossland formulations

Results show that the local approach does not lead to safe fatigue strength assessment because many points are located in the criterion failure zone. Since it takes into account the effect of defects, the non-local approach gives better results.

6. Conclusion

In this paper, the contribution of different effects: hardening, residual stresses and geometrical defects on the fatigue resistance of the studied alloy are quantified. Different characterization techniques were used to investigate these effects. Results show different types of defects, high tensile residual stresses and a strong material properties gradient locally on the edges (about 200 µm depth). To propose a fatigue design strategy for punched components, Crossland haigh cycle fatigue multiaxial strength criterion with its local and non-local formulations was used for the post-processing of FEA. Results show that the local approach does not lead to safe fatigue strength assessment. However, the non-local formulation gives better results.

References

[1] Achouri, M., Gildemyn, E., Germain, G., Dal Santo, P., Potiron A., 2014. Influence of the edge rounding process on the behaviour of blanked parts: numerical predictions with experimental correlation,» Int J Adv Manuf Technol., pp. Volume 71 Issue 5-8 (1019-1032).

[2] Lara, A., Picas, I., Casellas, D., 2013. Effect of the cutting process on the fatigue behaviour of press hardened and high strength dual phase steels. Journal of Materials Processing Technology, p. (213) 1908– 1919.

[3] Sanchez, L., Gutierrez-Solana, F., Pesquera, D., 2004. Fatigue behaviour of punched structural plates. Engineering Failure Analysis, p. 751–764.

[4] Maurel, V., Ossart, F., Billardon, R., 2003. Residual stresses in punched laminations: Phenomenological analysis. Journal of Applied Physics, pp. 93, 7106.

[5] Dehmani H., Brugger C., Palin-Luc T., Mareau C., Koechlin S., Experimental study of the impact of punching operations on the high cycle fatigue strength of Fe–Si thin sheets, International Journal of Fatigue, vol. 82, p. 721–729, 2016.
[6] Dehmani H., 2016, Experimental study of the impact of punching operations on the high cycle fatigue strength of Fe–Si thin sheets, PhD thesis Arts et Métiers ParisTech.
[7] C. Schayes, 2016, Low cycle fatigue of the Fe-3Si steel : damage mechanisms and strain localisation by EBSD, PhD thesis Université Lille 1
[8] Crossland. B., 1956. Effect of large hydrostatic pressures on the torsional fatigue strength of an alloy steel, Proc. Int. Conf. on Fatigue of Metals. Vol. 138. Institution of Mechanical Engineers London.
[9] ElMay, M., Saintier, N., Palin-Luc T., Devos, O., 2015. Non-local high cycle fatigue strength criterion for metallic materials with corrosion defects. Fatigue Fract Engng Mater Struct, vol. 38, p. 1017–1025.
[10] ElMay, M.,2013, Étude de la tenue en fatigue d'un acier inoxydable pour l'aéronautique en milieu marin corrosif, PhD thesis Arts et Métiers ParisTech.